Available online at www.sciencedirect.com
ScienceDirect
Ceramics International 38 (2012) 571–579
CERAMICS INTERNATIONAL
www.elsevier.com/locate/ceramint

Structure and properties of titania reinforced nano-hydroxyapatite/gelatin bio-composites for bone graft materials

C. Kailasanathan [a,1], N. Selvakumar [b,*], Vasant Naidu [c,1]

[a] Department of Mechanical Engineering, Sethu Institute of Technology, Pulloor, Kariapatti 626 115, Virudunagar District, Tamilnadu, India
[b] Department of Mechanical Engineering, Mepco Schlenk Engineering College, Sivakasi 626 005, Tamilnadu, India
[c] Department of Physics, Sethu Institute of Technology, Pulloor, Kariapatti 626 115, Virudunagar District, Tamilnadu, India

Received 6 May 2011; received in revised form 22 July 2011; accepted 22 July 2011
Available online 29th July 2011

Abstract

This work deals with the preparation of ceramic composites to be employed for the development of load bearing bone substitutes, made of inorganic minerals of needle like nano hydroxyapatite [nHAp: $Ca_{10}(PO_4)_6(OH)_2$] with bioinert titania as a reinforcing phase and gelatin as protein that mimic the natural bone exhibiting improved biomechanical features. As a monolithic, use of nHAp is limited for biomedical applications because of its inherent low fracture toughness and lack of flexibility. Hence, the incorporation of ceramics such as alumina, zirconia and titania is considered necessary to boost its mechanical properties. The composites of nHAp/TiO_2/gelatin in different weight percentage were prepared by phase separation technique. The identification and morphology of chemically synthesized nHAp particles were determined by XRD, FTIR and SEM analyses. The porosity of scaffolds varied from 77% to 82%. FTIR and XRD analyses showed the presence of molecular interactions and chemical linkages between nHAp particles, titania and gelatin matrix. The compressive strength of titania reinforced nanocomposites scaffolds could be elevated up to 10.15 MPa while those of nHAp/gelatin were 4.87 MPa. These results show that newly developed nHAp/TiO_2/gelatin composites may be superior for bone tissue engineering.

Keywords: FTIR; XRD; Nano biocomposites; Hydroxyapatite; Biomaterials

1. Introduction

The replacement or restoration of troubled, damaged, or lost bone is a major clinical problem worldwide. It has been estimated that about 6 million bone grafting procedures are done annually in the United State alone [1]. Present healing methods to treat bone loss or damage include use of bone grafts such as autograft and allograft. Even though autografts are considered as the gold standard for bone repair due to their optimal osteoconductive, osteoinductive, and osteogenic properties, they suffer from serious drawbacks such as added expense and pain to the patient and limited availability [2]. Allografts, although commercially available, have serious disadvantages such as risk of disease transfer. For that reason, there is a great need for the use of synthetic bone grafts; since the major structural component of natural bone (60%) is composed of an inorganic compound called hydroxyapatite (HAP) and organic component of type I collagen. The collagen phase gives form to the bone and contributes to its ability to resist bending, while the mineral component resists compression. The unique factors that contribute to the toughness of bone are the presence of nano-size apatite crystals, a dense network of collagen fibers. The combination of a hard inorganic material and an elastic hydrogel network provides unique mechanical properties to the bone. [3]. HAP has been investigated as a bone graft substitute [4]. However, HAP as well as the other calcium phosphate bone replacements behave like ceramics and are stiff due to their inorganic origin. Therefore, combinations of calcium phosphates and more elastic materials such as collagen or gelatin have been developed, though the maximum compressive strength of these composites obtained so far is 30 MPa, limiting their application to non-structural devices [5].

* Corresponding author. Tel.: +91 4562 235641.
E-mail addresses: uthrakailash@yahoo.co.in (C. Kailasanathan), nsk2966@yahoo.co.in (N. Selvakumar), drvasantnaidu@yahoo.com (V. Naidu).
[1] Tel.: +91 4566 308001.

0272-8842/$36.00
doi:10.1016/j.ceramint.2011.07.045

Further, a single-phase material also called monolithic does not always provide all the essential features required for bone growth. Therefore, there is a great need for engineering multi-phase materials also called composite with structure and composition similar to natural bone [6]. A hydroxyapatite–gelatin nanocomposite fabricated via phase inversion technique not only mimics the biochemistry and nanostructures of bone but also supports the attachment, proliferation and differentiation of osteoblasts [4]. Gelatin possesses important characteristics which favor it for use as a biomaterial: high tensile strength, high affinity for water, low antigenicity, hemostatic properties, controllable biodegradation, low inflammatory and cytotoxic properties and the ability to promote cellular attachment, growth and differentiation [7]. Improvement of the mechanical properties can be achieved by the addition of oxide phases, e.g. alumina, titania, zirconia, etc. [8]. The selection of appropriate material for the reinforcement to produce the composite scaffold to be used in bone grafting is critically important, since its properties will determine the properties of the composite. Titania is added to nHAp/gelatin composite in order to obtain high fracture toughness, high porosity, and excellent biocompatibility [9,10]. In this work, the attempt is made to fabricate a nano biocomposite scaffold nHAp/gelatin and nHAp/titania/gelatin that duplicate natural bone in structure and properties. In the first step, needle-like nHAp particles were synthesized using wet chemical method. In the following steps, pure gelatin scaffold and scaffolds comprising different contents of nHAp, titania particles in the gelatin matrix were fabricated using phase separation method. The porous scaffold fabricated by this method showed intense structural features. To evaluate synthesized nHAp and produced scaffolds morphology, chemical composition and crystalline structure, FTIR, XRD and SEM analysis were used. The mechanical properties were determined using an Instron type machine.

2. Materials and methods

2.1. Chemicals

Deionized water was used in all reactions. The sodium hydroxide [NaOH] pellets were used as purchased (Merck) to prepare NaOH solution. Analytical grade of diammonium hydrogen phosphate [$(NH_4)_2HPO_4$], dioxane, gelatin, titania and calcium nitrate [$Ca(NO_3)_2{\cdot}4H_2O$] were used as supplied (Merck).

2.2. Synthesis of nHAp powder

The nanoparticles prepared by electro-reduction processes [11] are formed as spongy layers that can be easily separated to give fine particles and a novel laser–liquid–solid interaction (LLSI) technique [12] is also used to prepare nanomaterials in the form of particles, rods, and tubes from liquid precursors. Pure and cobalt-exchanged hydroxyapatite (HAp and CoHAp) powders are synthesized by hydrothermal method [13]. A sol–gel auto combustion route and wet chemical method have been suggested to synthesize nano powders in order to obtain fine crystal size [14]. In this study, the nHAp nanocrystals were synthesized by wet chemical method [15]. In this method, 0.03 M aqueous solution of diammonium hydrogen phosphate was added drop wise to 0.05 M aqueous solution of $Ca(NO_3)_2{\cdot}4H_2O$ as P and Ca precursors respectively. Before mixing, the pH value of $Ca(NO_3)_2{\cdot}4H_2O$ solution was adjusted to 11 by adding sodium hydroxide solution and the temperature was maintained at $70 \pm 5\ ^\circ C$. The precipitated nHAp mixture was aged for 24 h at room temperature and centrifuged at the rotation speed of 9000 rpm for 0.5 h in a Remi rotor. Then the powder was frozen at $-20\ ^\circ C$ for 1 h and dried in freeze dryer system at $-75\ ^\circ C$ for 1 week and calcined at $600\ ^\circ C$ for 1 h.

2.3. Synthesis of nHAp/gelatin and nHAp/TiO_2/gelatin composites

Porous objects of hydroxyapatite composites may be prepared by mixing sodium chloride as channeling agent with ultra-high molecular weight polyethylene as a binder [16]. In this work, the nHAp/gelatin composite scaffolds were fabricated using a phase separation technique [17]. Briefly, the HAP nanocrystals powder was dispersed in a solvent by sonication for 30 s at 15 W (Virsonic 100, Cardiner, NY). After that, gelatin was dissolved in the nHAp suspended solvent at about $60\ ^\circ C$ to make homogeneous solutions with desired concentrations. 2.5 ml gelatin/nHAp mixture was added into a Teflon vial, sonicated again and then transferred into a freezer at a preset temperature to induce solid–liquid or liquid–liquid phase separation. The solidified mixture was maintained at that temperature overnight and then transferred into a freeze-drying container which was maintained at a temperature between 5 °C and 10 °C by salt–ice bath for freeze drying. The samples were freeze-dried at 0.5 mmHg for 7 days to remove solvent. Then the samples were dried in air for 1 week. Similarly, titania was added to nHAp with the ratio (nHAp: TiO_2 = 50:10, 40:20, 30:30 and 20:40) along with 40% gelatin. Thus, different nHAp/TiO_2/gelatin composites with different weight% were prepared.

2.4. Characterization

2.4.1. FTIR analysis

The Fourier transform infrared (FTIR) spectra were collected for the powders using a Bruker Optics FTIR spectrometer, Germany. Spectra were obtained at $4\ cm^{-1}$ resolution, averaging 24 numbers of scans.

2.4.2. XRD analysis

X-ray powder diffraction (XRD) patterns were obtained for the powder samples using PANalytical X'per PRO difractometer using Cu-Kα radiation (λ = 0.15418 nm). Data were collected over the 2θ range 10–90° with a step size of 0.0170° and step time of 15.5076 s.

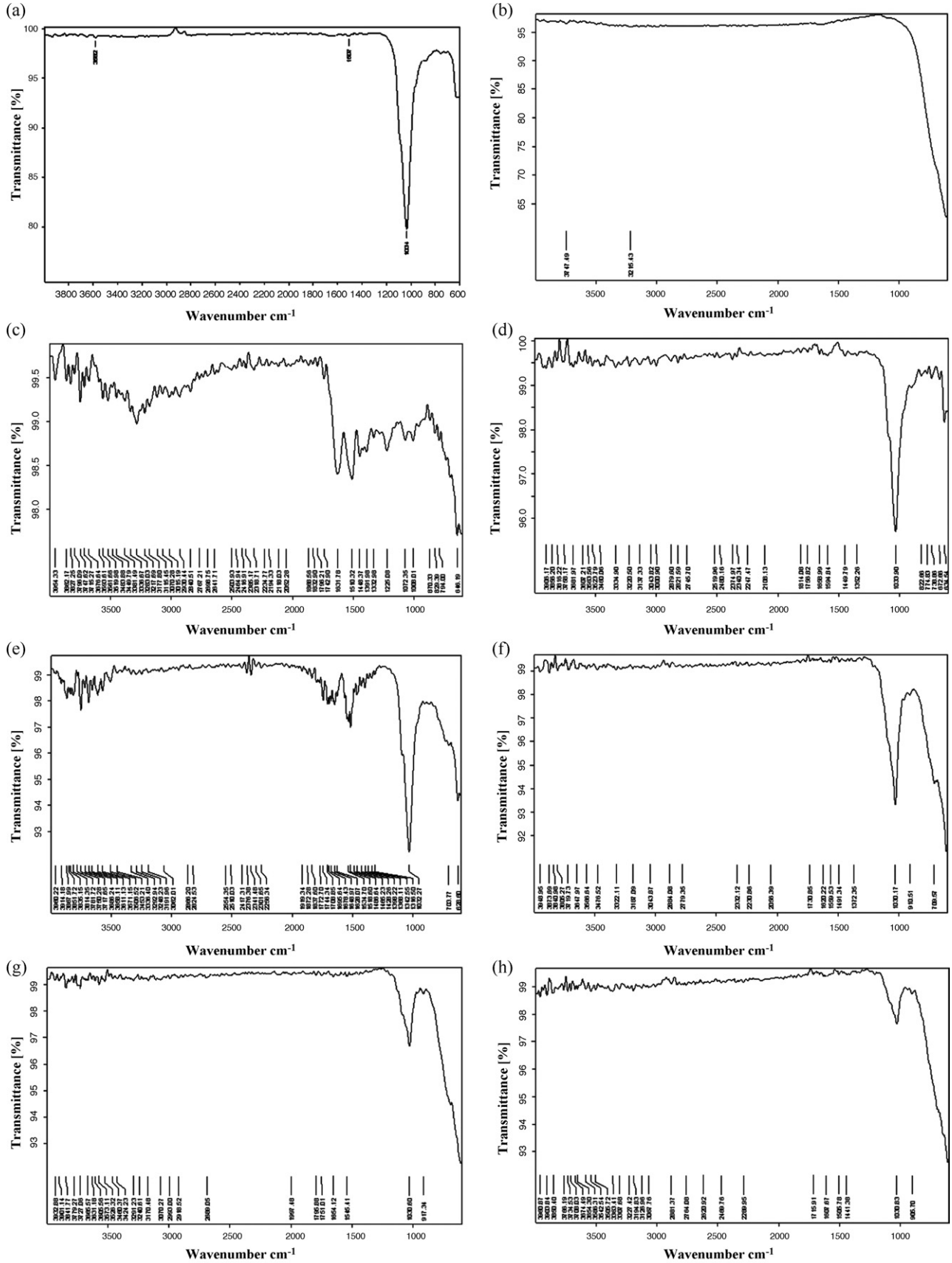

Fig. 1. FTIR spectra of (a) nHAp, (b) titania, (c) pure gelatin, (d) nHAp/gelatin (60:40), and (e–h) nHAp:titania:gelatin: (e) (50:10:40), (f) (40:20:40), (g) (30:30:40), and (h) (20:40:40).

2.4.3. SEM analysis

The morphology of the synthesized nHAp and composite scaffolds was observed by scanning electron microscopy (SEM, Make: Hitachi, Japan, Model: SU510). Prior to examination, each sample was ion sputtered with gold to enhance charging of particles.

2.4.4. Porosity measurement

The porosity may be measured by a destructive gravimetric technique [18] and conventional liquid substitution method [19]. In liquid substitution method, ethanol was used as the displacing liquid because it penetrated easily into the pores of the scaffold, but not into the composite itself. Briefly, a sample of measured weight W was immersed in a graduated cylinder containing a known volume (v_1) of ethanol and kept for 24 h to allow the ethanol to penetrate into the pores of the scaffold. The total volume of the remaining ethanol and the ethanol-impregnated scaffolds was then recorded as v_2 by simply reading the level in the cylinder. The volume difference ($v_2 - v_1$) represents the volume of the scaffolds material. The ethanol impregnated scaffolds were then removed from the graduated cylinder and the residual ethanol volume was recorded as v_3. Hence the total volume of the scaffolds was $v = v_2 - v_3$ and the bulk density of the scaffold were expressed as:

$$\rho = \frac{w}{v_2 - v_3}$$

By measuring the initial and final weights w_i and w_f, respectively, of the scaffolds after soaking in ethanol ($\rho_{ethanol} = 0.789\ g/cm^3$) for 24 h; the pore volume of the composite scaffold can be calculated as $(w_f - w_i)/\rho_{ethanol}$. Then the porosity can be measured using the following equation:

$$\text{Porosity} = \frac{w_f - w_i}{\rho_{ethanol}} \left(\frac{1}{v_2 - v_1} \right)$$

At least five scaffolds were tested for each sample and the average porosity reported.

2.5. Mechanical property

The compressive strength and modulus of the composite scaffolds were determined using a mechanical testing machine (TIRA Test-2720). According to ASTM D 5024-95 standard, cylindrical samples were prepared with diameters of 26 mm and lengths twice its diameter. The cross-head speed was set at 0.5 mm/min, and the load was applied until the specimen was failed. The compressive modulus was calculated as the slope of the initial linear portion of the load–displacement curve. The ultimate compressive strength and modulus was determined from the load–displacement curve.

3. Results and discussion

3.1. FTIR analysis

To evaluate the functional groups of the synthesized nHAp powder, titania, gelatin and nHAp/gelatin composite scaffolds, FTIR analysis was first employed as shown in Fig. 1. The

Table 1
Characteristic wave numbers of nHAp, titania, pure gelatin, nHAp/gelatin and nHAp/TiO_2/gelatin.

Characteristic group	nHAp (cm^{-1})	TiO_2 (cm^{-1})	Gelatin (cm^{-1})	nHAp/gelatin (cm^{-1})	nHAp/TiO_2/gelatin (cm^{-1})
$-PO_4^{3-}$	600			634	628
	952			954	960
	1034			1033	1032
	1090			1089	1096
$-OH^-$	627			622	630
	3582			3563	3571
		3215			3248
		3747			3750
CO_3^{2-}	873			870	875
	1421			1419	1428
	1457			1450	1465
Absorbed water	1631			1630	1637
Lattice water	3410			3415	3425
–C=O			1631	1635	1628
		2187			2190
		2209			2215
CH– stretching vibration			2767	2746	2742
			2840	2822	2819
			2930	2991	2866
–OH– in –COOH			3217-3593	Disappeared	Disappeared
$-CH_3$	–		1391	1352	1398
			1448	1450	1428
Ti–O		Below 700			Below 700

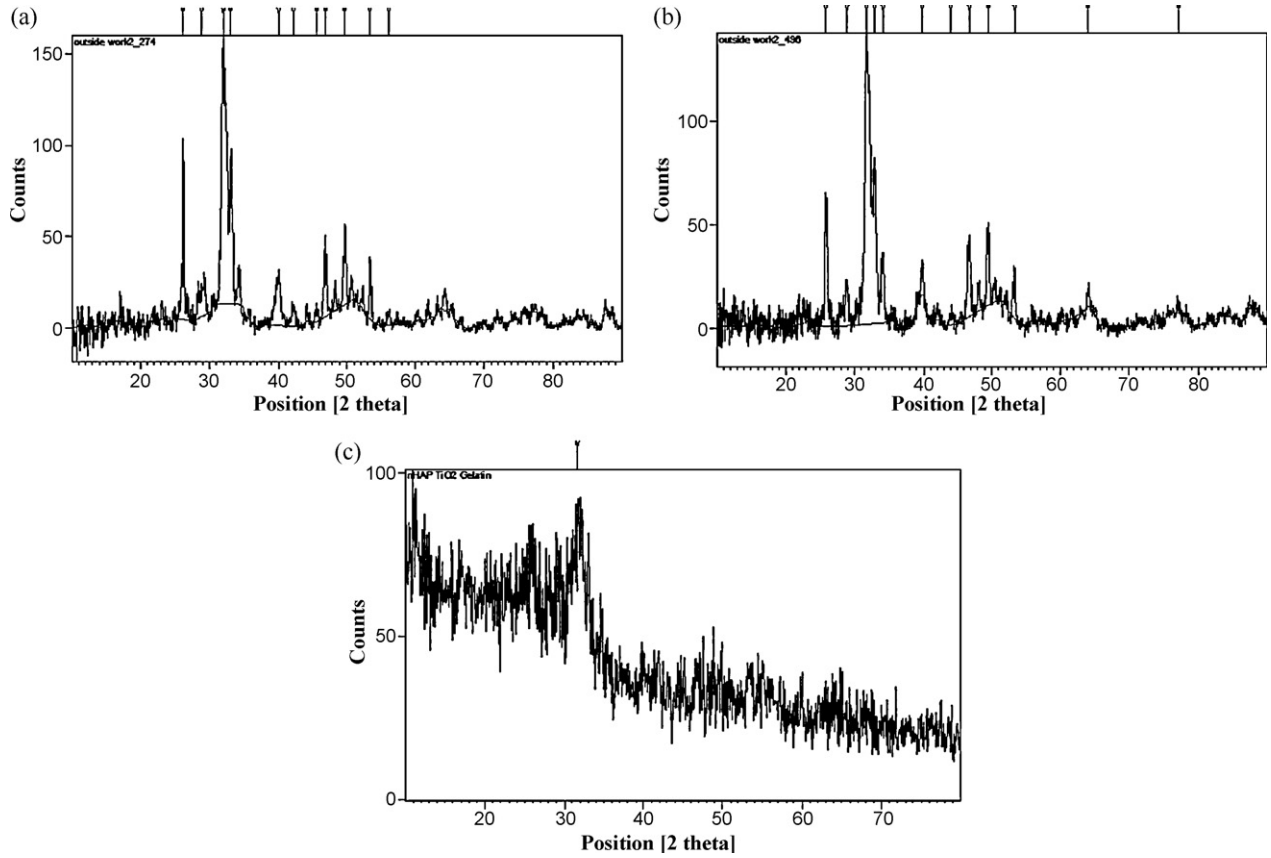

Fig. 2. XRD pattern of (a) nHAp, (b) nHAp/gelatin, and (c) nHAp/TiO_2/gelatin.

corresponding wave numbers of characteristic groups of titania, pure gelatin (Fig. 1(a) and (b)), nHAp, nHAp/gelatin and nHAp/TiO_2/gelatin are listed in Table 1. FTIR analysis in Fig. 1 shows some variations in adsorption peaks of the nHAp, gelatin and the nano composite.

Saturated peak of TiO_2 (Fig. 1(b)) below 700 cm^{-1} is assigned to Ti–O and Ti–O–Ti bonding of titania. The small peak at 3215 and 3747 cm^{-1} is attributed to stretching of –OH groups in the powder.

PO_4^{3-} peaks of the nHAp (Fig. 1(a)) at 600, 952, 1033 and 1090 cm^{-1}, move back to in the nano composite nHAp/gelatin 634, 954, 1033 and 1089 cm^{-1} (Fig. 1(d)) and to 628, 960, 1032 and 1096 cm^{-1} in the nHAp/TiO_2/gelatin composite (Fig. 1(e)). The data showed that a process of dehydroxylation and rehydroxylation might have occurred in the composite. Furthermore, the wave number of –CH vibration peaks at 2930, 2840 and 2767 cm^{-1} in the gelatin spectrum (Fig. 1(c)) shifted to 2911, 2822, 2746 cm^{-1} in the nano composite nHAp/gelatin (Fig. 1(d)), but reduced to 2866, 2824 and 2749 cm^{-1} in the nHAp/TiO_2/gelatin composite (Fig. 1(e)). These results indicate some molecular interactions between the nHAp and gelatin in the nano composite.

The intensity of –OH– absorption peaks at 3582 and 627 cm^{-1} in the nHAp decreases obviously in the nano composite. The –C═O vibration peak of gelatin at 1631 cm^{-1} shifts to 1635 cm^{-1} and 1628cm^{-1} in the nano composite and nHAp/TiO_2/gelatin composites respectively. These changes may be attributed to the formation of hydrogen bonding between –OH– group of nHAp and –C═O group of gelatin in the nano composite.

The stretching vibration peak of OH– in carboxyl groups (–COOH) of gelatin at 3593 cm^{-1} disappeared. It can be assumed that carboxyl groups (–COOH) of gelatin were ionized to form –COO– ions during the composite formation. The FTIR spectra (Fig. 1(e)–(h)) of nano composites with different proportion of nHAp, titania and gelatin show no variations in the peaks of intensity of functional groups.

3.2. XRD analysis

XRD analysis results of the nHAp, nHAp/gelatin composite and nHAp/TiO_2/gelatin are shown in Fig. 2(a)–(c). Comparison of nHAp (a) with that of the composite (b and c), the peaks' position of the starting nHAp does not change in the composite. This means that the nHAp still keeps its original crystal structure in the composite. It can be observed in (b) and (c) that there are two characteristic peaks of gelatin at $2\theta = 49^\circ$ and 64°. It can be obtained from (b) and (c) that the crystallinity of gelatin and titania in the composite is 34% and 25%, respectively. The decrease of crystallinity of gelatin in composite indicates that the crystal structure of gelatin changed after forming composite with nHAp, which may result from the interfacial chemical bonding formed between nHAp, titania and gelatin. Combining IR and XRD analysis, it can be deduced

that molecular interaction and chemical bonding may be presented between nHAp, titania and gelatin in the composite, which may greatly affect the properties of the composite.

3.3. SEM analysis

The morphology and nanostructure of the scaffolds are examined using SEM and shown in Fig. 3. SEM micrograph of the synthesized nHAp prepared at 70 ± 5 °C with 24 h aging time is shown in Fig. 3(d). It shows needle like morphology with particle width ranging from 100 to 175 nm and the length of 100–400 nm. The nHAp particles obtained by the wet chemical method appear as white colour, bouncy and free flowing powders. From the micrograph (Fig. 3(d)), it is inferred that most of the particles are of single crystals, needle-like shape with no agglomeration. Due to the effect of drying small sections of precipitate and less opportunity for particles to agglomerate in freeze drying, it reveals that the powder is interconnected by macro and micro-pores inside and this will enhance protein absorption on pore surface to facilitate bone formation.

The pale yellowish nano composite nHAp/gelatin scaffold (Fig. 3(e) and (f)) maintains a regular internal ladder-like pore

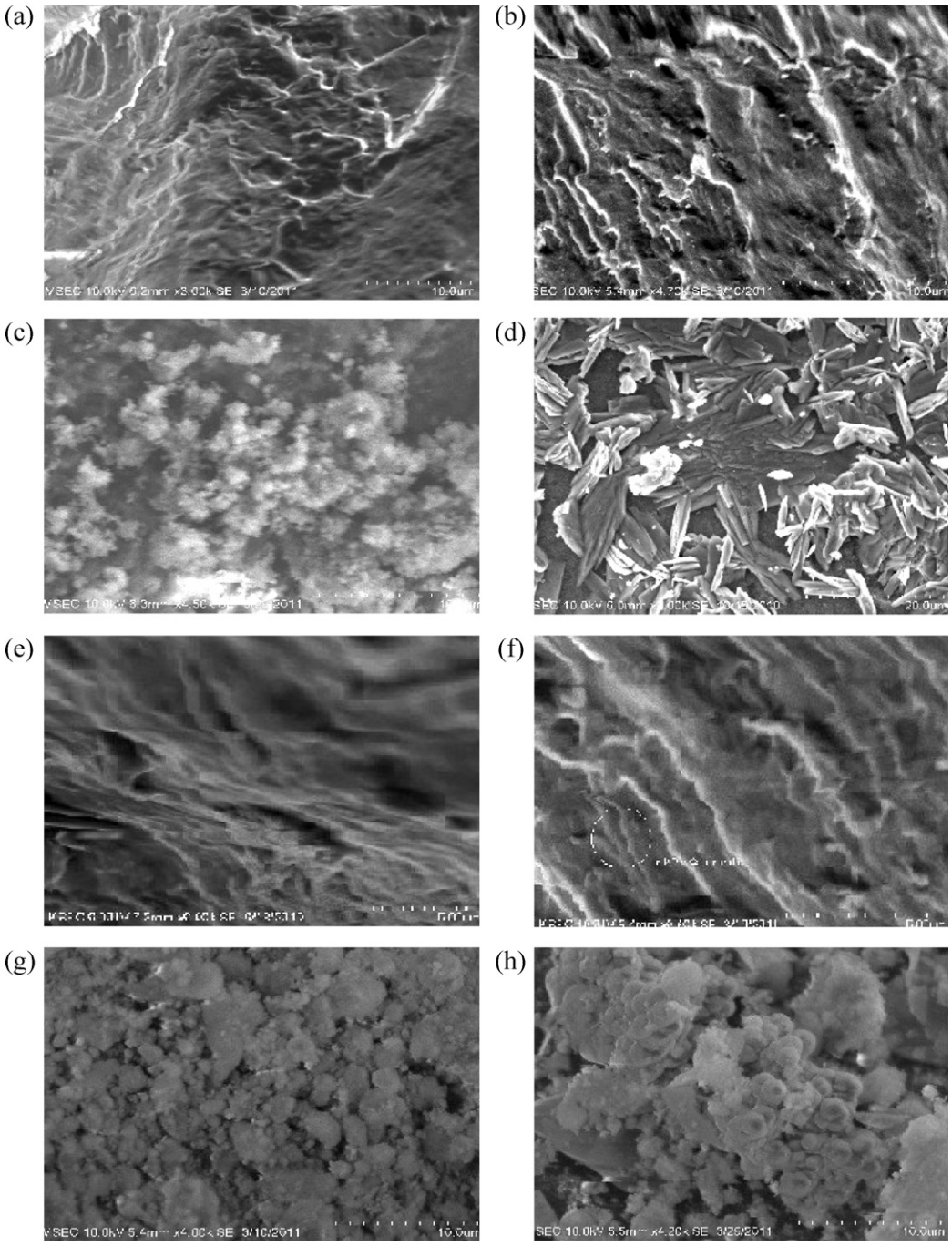

Fig. 3. SEM images of (a and b) gelatin, (c) titania, (d) nHAp, (e and f) nanocomposites scaffold nHAp/gelatin, (g and h) nHAp/titania/gelatin obtained at (a, e and g) low and (b, f and h) high magnifications.

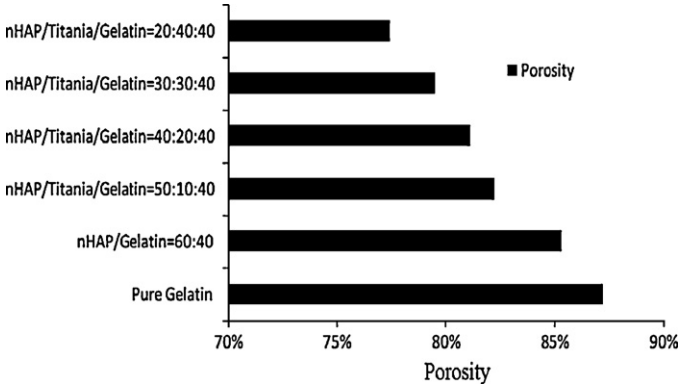

Fig. 4. Porosity content of pure gelatin, nHAp/gelatin and nHAp/titania/gelatin scaffolds.

structure similar to pure gelatin scaffold (Fig. 3(a) and (b)). Micrographs' comparison of the gelatin and nHAp/gelatin scaffolds (Fig. 3(a) and (e)) reveals no definite morphological differences. Needle-like nHAp particles are distributed within the pore walls of the nanocomposite scaffold and no aggregation appears in pores (Fig. 3(e) and (f)). The physical appearances of the nHAp/TiO_2/gelatin scaffold (Fig. 3(g) and (h)) are quite different from starting materials (Fig. 3(a)–(d)). It is found that the nHAp and titania particles are aggregated into large clusters and fixed in the gelatin matrix. The composites reveal the formation of large pores on their surfaces but the pores are not uniform.

In this study, a homogeneous system made by mixing nHAp/TiO_2/gelatin composite powder with ethanol was phase separated by heating the system up to 50 °C, at which temperature the phase change of ethanol occurred. This phase change from liquid ethanol to gaseous one gave rise to a large number of gaseous nuclei uniformly distributed in the mixture. Following a nucleation and growth mechanism, these nuclei gradually grew bigger and bigger and finally formed an interconnective porous structure.

3.4. Porosity

The average porosity of all scaffolds is shown in Fig. 4. A high degree of porosity would make easy the transfer of nutrients and excretion of the waste products, and the scaffold should have high tensile strength and high toughness in order to be consistent with human tissues [20]. The porosity of pure gelatin scaffolds (87.2%) decreases by addition of nHAp content in nHAp/gelatin scaffold (85.3%). The porosity of nHAp/Tio_2/Gelatin scaffolds of different weight percentage gradually decreases from 82.2% to 77.4%. nHAp and titania particles may be likely to fill the available space in pores of gelatin and reduce the porosity of scaffolds. The effect of the titania particles on the porosity is not close to that of the nHAp particles. All scaffolds reveal high porosity levels of at least 77% containing interconnected pore structure. This suggests that the phase separation method is a practical method for preparing high porosity polymer scaffolds. These porous scaffolds may facilitate cell growth and survival.

3.5. Mechanical property

The mechanical test was performed on the nHAp/gelatin and nHAp/TiO_2/gelatin composite scaffolds. The compressive strength and modulus of nHAp/TiO_2/gelatin scaffolds increased with titania content (Table 2). Representative load–displacement curves for each composition are provided in Fig. 5(a)–(f). The pure nHAp exhibits low compressive strength of about 2 MPa as seen from Fig. 5(f). The addition of even 40% gelatin results in a remarkable increase in the compressive strength by a factor of about 2.5. The nHAp/gelatin scaffold prepared using phase separation technique had a compressive modulus of 0.47 GPa and it was raised to 1.46 GPa when titania was introduced as a reinforcing element. The addition of titania into the scaffold improved the mechanical properties. The compressive strength increased significantly to 5.92 MPa when the titania proportion reached 30% of the composite and reached 10.15 MPa when the ratio of nHAp, titania to gelatin was 20:40:40 (Fig. 5(a)–(f)). When the porosities of the scaffolds varied from approximately 77–85%, the compressive strength of the composites gradually decreased from 10.15 to 4.67 MPa, and the modulus from 1.46 to 0.47 GPa. Because of high porosity, it is difficult to achieve high compressive strength for porous materials [21]. So it is realized that the compressive strength and modulus decreased with the growth of scaffold's porosity.

While there is no clearly distinct standard of the balance between porosity and mechanical strength required, the scaffolding material should have mechanical strength as close as possible to the strength of cancellous bone. The composite scaffold with high porosity is chosen in favor of cell growth and proliferation, but achieved at the expense of the decrease of

Table 2
Mechanical properties of composite scaffolds.

Composite scafffolds	Weight ratio	Mechanical properties		
		Porosity (%)	Compressive strength (MPa)	Compressive modulus (GPa)
nHAp		–	1.94	0.15
nHAp/gelatin	60:40	85.3	4.67	0.47
nHAp/TiO_2/gelatin	50:10:40	82.2	4.87	0.47
nHAp/TiO_2/gelatin	40:30:40	81.1	5.51	0.49
nHAp/TiO_2/gelatin	30:30:40	79.5	5.92	0.53
nHAp/TiO_2/gelatin	20:40:40	77.4	10.15	1.46

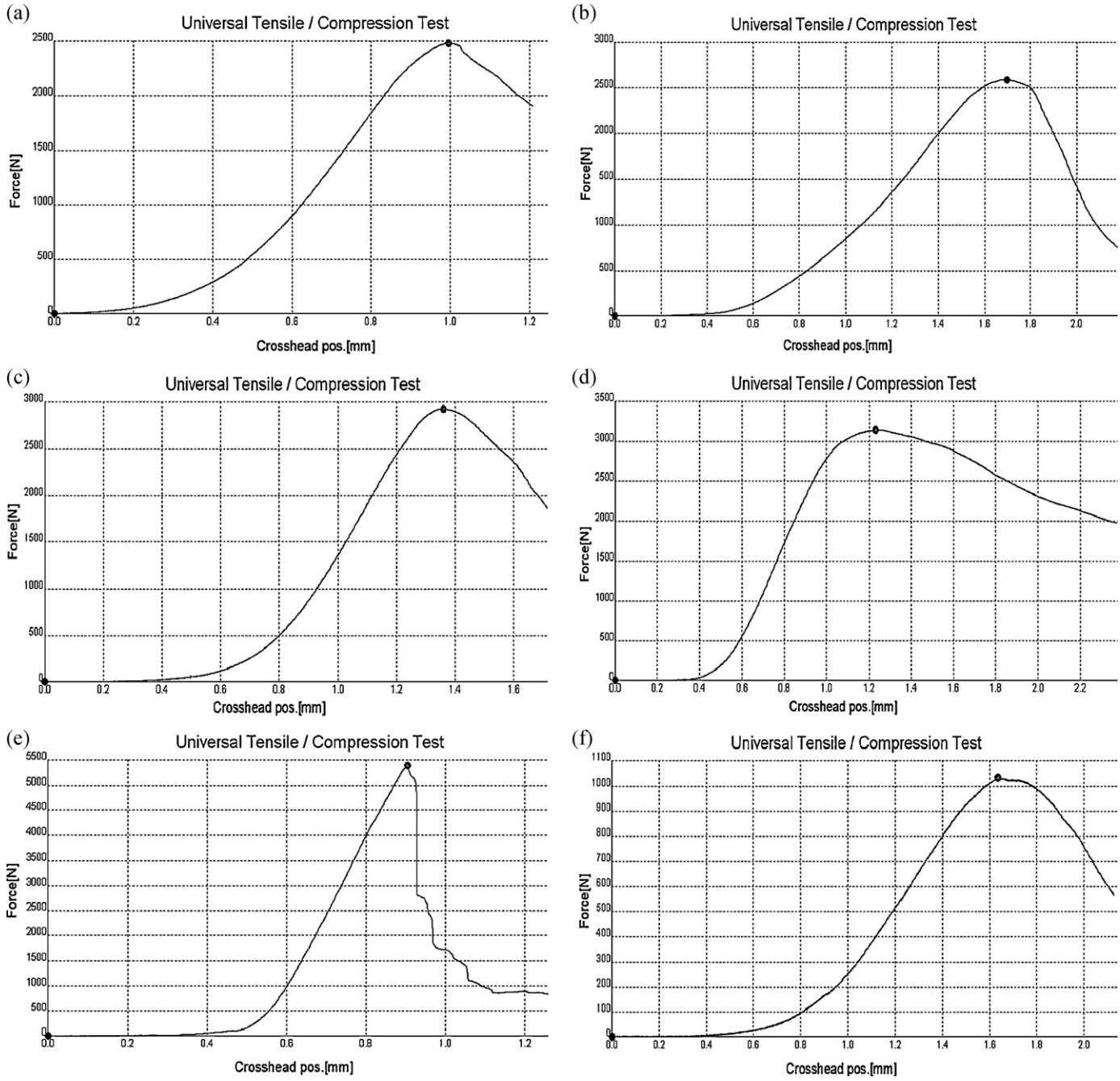

Fig. 5. Curves showing compressive strength of nano composites of (a) nHAp/gelatin (60:40), (b) nHAp/titania/gelatin (50:10:40), (c) nHAp/titania/gelatin (40:20:40), (d) nHAp/titania/gelatin (30:30:40), (e) nHAp/titania/gelatin (30:30:40), and (f) nHAp.

mechanical strength. Mechanical test results of the nHAp/TiO_2/gelatin scaffolds show that the composite scaffolds have a compressive strength of 10.15 MPa, similar to the upper value of the strength of cancellous bone, with the porosity of about 77%, which has been regarded as the lowest porosity required. The strength of porous scaffold materials mainly depends on the uniform distribution of stiff nano-scale HAp granules and titania in the soft gelatin matrix. The gelatin content had a significant effect on the scaffold structure and proved to be a highly important parameter affecting the mechanical properties of the composites. Pure nHAp is brittle, but a distinct deformability is obtained due to the presence of the organic matrix.

4. Conclusions

The present study investigated new nHAp/TiO_2/gelatin composite scaffolds developed using phase separation technique. The gelatin content had a significant effect on the scaffold structure and proved to be a highly important parameter affecting the mechanical properties of the composites. Pure nHAp is brittle, but a distinct deformability is gained due to the

presence of the organic matrix. Nano-sized HAp particles and titania were successfully incorporated into the gelatin matrix. The nHAp/titania/gelatin composite showed higher compressive strength (10.15 MPa) with porosity of 77.4% than did nHAp/gelatin scaffold and modulus increased linearly with increase of TiO_2 content. The compressive strength of the scaffolds is compared to the compressive strength of the cancellous bone. The results indicate that the composites of the system nHAp–titania–gelatin are suitable for further development and could be valuable for the fabrication of bone-substitution materials with adjustable mechanical properties.

References

[1] R.W. Bucholz, Nonallograft osteoconductive bone graft substitutes, Clin. Orthop. 398 (2002) 44–52.

[2] A.R. Gupta, N.R. Shah, T.C. Patel, J.N. Grauer, Perioperative and long-term complications of lliac crest bone graft harvesting for spinal surgery: a quantitative review of literature, Int. Med. J. 8 (2001) 163–166.

[3] G.E. Fantner, H. Birkedal, J.H. Kindt, T. Hassenkam, J.C. Weaver, J.A. Cutroni, B.L. Bosma, L. Bawazer, M.M. Finch, G.A. Cidade, D.E. Morse, G.D. Stucky, P.K. Hansma, Influence of the degradation of the organic matrix on the microscopic fracture behavior of trabecular bone, Bone 35 (2004) 1013–1022.

[4] C.C. Ko, Y.-L. Wu, W.H. Douglas, R. Narayanan, W.-S. Hu, In vitro and in vivo tests of hydroxyapatite–gelatin nanocomposites for bone regeneration: a preliminary report, Mater. Res. Soc. Symp. Proc. (2004) 823.

[5] L.L. Hench, J.M. Polak, Third-generation biomedical materials, Science 295 (5557) (2002) 1014–1017.

[6] R. Murugan, S. Ramakrishna, Development of nanocomposites for bone grafting, Compos. Sci. Technol. 65 (2005) 2385–2406.

[7] H. Sascha, H. Christiane, B. Ricardo, R. Antje, N. Berthold, M. Michael, W. Hartmut, H. Thomas, Bioactive silica–collagen composite xerogels modified by calcium phosphate phases with adjustable mechanical properties for bone replacement, Acta Biomater. 5 (2009) 1979–1990.

[8] K. Prabakaran, S. Kannan, S. Rajeswari, Development and characterisation of zirconia and hydroxyapatite composites for orthopaedic applications, Trends Biomater. Artif. Organs 18 (2) (2005).

[9] H. Li, K.A. Khor, P. Cheang, Titanium dioxide reinforced hydroxyapatite coatings deposited by high velocity oxy-fuel (HVOF) spray, J. Biomater. 24 (2002) 85–91.

[10] M.P. Lexis, W.R. Joel, J.S. Malcom, M. Sayer, Silicon substitution in the calcium phosphate bioceramics, Biomaterials 28 (2007) 4023–4032.

[11] M. Raja, J. Subha, F. Binti Ali, S.H. Ryu, Synthesis of copper nanoparticles by electroreduction process, Mater. Manuf. Process. 23 (8) (2008) 782–785.

[12] D. Jogender Singh, T. Poondi, M. Obbins, M. Pietro, Novel nanomaterials synthesis by laser–liquid–solid interaction, Mater. Manuf. Process. 23 (3) (2008) 228–240.

[13] S. Zoran, V. Ljiljana, M. Smilja, I. Nenad, U. Dragan, Hydrothermal synthesis of nanosized pure and cobalt-exchanged hydroxyapatite, Mater. Manuf. Process. 24 (10–11) (2009) 1096–1103.

[14] J. Chandradass, M. Balasubramanian, K.H. Kim, Synthesis and characterization of $LaAlO_3$ nanopowders by various fuels, Mater. Manuf. Process. 21 (2) (2006) 211–218.

[15] C. Kailasanathan, N. Selvakumar, K. JeyaSubramanian, Effect of calcination in synthesis of nano hydroxyapatite for bone grafting, Mater. Manuf. Process. (2011), doi:10.1080/10426914.2011.577874.

[16] K. Pal, S. Pal, Development of porous hydroxyapatite scaffolds, Mater. Manuf. Process. 21 (3) (2006) 325–328.

[17] R. Zhang, P.X. Ma, Poly(alpha-hydroxyl acids)/hydroxyapatite porous composites for bone tissue engineering. I. Preparation and morphology, J. Biomed. Mater. Res. 44 (1999) 446–455.

[18] M. Ray, S. Ganguly, M. Das, S. Datta, N.R. Bandyopadhyay, S.M. Hossain, Artificial neural network (ANN)-based model for in situ prediction of porosity of nanostructured porous silicon, Mater. Manuf. Process. 24 (1) (2009) 83–87.

[19] E. Nejati, V. Firouzdor, M.B. Eslaminejad, F. Bagheri, Needle-like nano hydroxyapatite/poly(L-lactide acid) composite scaffold for bone tissue engineering application, Mater. Sci. Eng. C 29 (3) (2009) 942–949.

[20] B. Avinash, W. Shing-Chung, T.S. Srivatsan, O.N. Glen, M. Garima, Processing methodologies for polycaprolactone–hydroxyapatite composites: a review, Mater. Manuf. Process. 21 (2) (2006) 211–218.

[21] W. Huanan, L. Yubao, Z. Yi, L. Jihua, M. Sansi, C. Lin, Biocompatibility and osteogenesis of biomimetic nano-hydroxyapatite/polyamide composite scaffolds for bone tissue engineering, Biomaterials 28 (2007) 3338–3348.